

On the true fractions of repeating and non-repeating FRB sources

SHUNKE AI,¹ HE GAO,² AND BING ZHANG¹

¹*Department of Physics and Astronomy, University of Nevada Las Vegas, Las Vegas, NV 89154, USA*
ais1@unlv.nevada.edu, zhang@physics.unlv.edu

²*Department of Astronomy, Beijing Normal University, Beijing 100875, People's Republic of China; gaohe@bnu.edu.cn*

(Received —; Revised —; Accepted —)

ABSTRACT

Observationally, fast radio bursts (FRBs) can be divided into repeating and apparently non-repeating (one-off) ones. It is unclear whether all FRBs repeat and whether there are genuine non-repeating FRBs. We attempt to address these questions using Monte Carlo simulations. We define a parameter T_c at which the accumulated number of non-repeating sources becomes comparable to the total number of the repeating sources, which is a good proxy to denote the intrinsic repeater fraction among FRBs. Assuming that both types of sources exist, we investigate how the *observed* repeater fraction evolves with time for different parameters, including T_c , the repeating rate distribution power-law index q , the minimum repetition rate $r_{0,\min}$, as well as the Weibull distribution index k for repeating bursts. We find that unless $T_c \rightarrow \infty$ (i.e. there is no genuine non-repeating FRB source), the observed repeater fraction should increase with time first, reaching a peak, and then declines. The peak time T_p and the peak fraction $F_{r,\text{obs},p}$ depend on T_c and other repeating rate parameters. With the current data, one may pose a lower limit $T_c > (0.5 - 25)$ d for reasonable parameter values. Future continuous monitoring of FRBs using wide-field radio telescopes such as CHIME would measure or set a more stringent lower limit on T_c . The detection of a peak in the observed repeater fraction would disfavor the ansatz that “all FRB sources repeat”.

Keywords: fast radio burst

1. INTRODUCTION

Fast radio bursts (FRBs) are mysterious transients originating from distant universe (Lorimer et al. 2007; Thornton et al. 2013; Petroff et al. 2019; Cordes & Chatterjee 2019). Even though early observations only detected one-off events, the discovery of multiple bursts from FRB 121102 (Spitler et al. 2016) suggested that at least some are repeating sources. Recent observations by CHIME revealed that repeating FRBs are commonly observed (CHIME/FRB Collaboration et al. 2019a,b).

One intriguing question is whether there exist genuinely non-repeating FRBs. The difficulty in addressing this problems lies in the wide range of the repeating waiting times (Palaniswamy et al. 2018; Caleb et al. 2019) and FRB luminosities (Luo et al. 2018, 2020; Lu & Piro 2019). It is highly likely that some apparently non-repeating FRBs are actually repeaters. The non-detection of the repeated bursts could be because of the long waiting time or low flux of the repeating bursts (Palaniswamy et al. 2018). The high event

rate of FRBs may suggest that the majority of FRBs are repeaters (Ravi 2019). On the other hand, deep follow up observations of some FRBs (e.g. the famous “Lorimer” event) did not reveal repeated bursts (Petroff et al. 2015). Palaniswamy et al. (2018) and Caleb et al. (2019) argued that active repeaters such as FRB 121102 are abnormally active. If all FRBs are similar to FRB 121102, many one-off bursts should have been detected as repeaters.

However, repeating FRBs may have different degrees of repetition level. If FRBs have a wide range of repetition rate, it is possible that the ansatz “all FRB sources repeat” is true (e.g. Lu et al. 2020). Are there indeed genuine non-repeaters? If so, how can we find out that they exist? What are the true fractions of repeaters and non-repeaters?

In this *Letter*, we attempt to address these questions through Monte Carlo simulations. The basic formalism of our approach is described in Section 2. The simulation methodology is outlined in Section 3 and the results are

presented in Section 4. Section 5 is conclusions with some discussion.

2. BASIC FORMALISM

A repeating FRB source can produce a sequence of bursts, but only those with energy exceeding a threshold value are detectable. Below we follow [Lu et al. \(2020\)](#) to calculate the repeating rate of repeaters but add a population of genuine non-repeaters. We assume that the threshold fluence for a detector to trigger an FRB event is F_{th} . For a source at the luminosity distance D_L , the threshold energy for a burst to be detectable is

$$E_{\text{th}} = 4\pi D_L^2 F_{\text{th}} (1+z)^{\alpha-1}, \quad (1)$$

where an k -correction has been introduced and α is the intrinsic spectral index of the burst ($S_\nu \propto \nu^{-\alpha}$), with $\alpha = 1.5$ adopted.

Consider that the repeating rate of a repeating FRB source is related to the intrinsic energies of the bursts as a power-law function, i.e.

$$\frac{dr}{dE} = \frac{r_0}{E_0} \left(\frac{E}{E_0} \right)^{-\gamma} \exp \left(-\frac{E}{E_{\text{max}}} \right) \quad (2)$$

where $\gamma = 1.92$ is inferred from the current repeating FRB sample ([Lu et al. 2020](#)). We set $E_0 = 10^{30} \text{ erg Hz}^{-1}$ and $E_{\text{max}} = 10^{34} \text{ erg Hz}^{-1}$ ([Lu & Piro 2019](#)). Here r_0 is a normalization parameter, which stands for the intrinsic repeating rate of the bursts at $E = E_0$. For FRB121102, the measured value is $r_0 = 0.1 \text{ hr}^{-1}$ ([Law et al. 2017](#); [James 2019](#)). Then, the effective repeating rate of bursts above E_{th} could be calculated as

$$r(> E_{th}) = r_0 \int_{x_{th}}^{\infty} dx x^{-\gamma} \exp \left(\frac{-xE_0}{E_{\text{max}}} \right). \quad (3)$$

where $x = E/E_0$ and $x_{th} = E_{th}/E_0$.

As a function of r , the distribution of time intervals (δ) between two adjacent bursts could be described by a Weibull probability density function ([Oppermann et al. 2018](#)), which reads

$$\mathcal{W}(\delta|k, r) = k\delta^{-1} [\delta r \Gamma(1 + 1/k)]^k e^{-[\delta r \Gamma(1 + 1/k)]^k}, \quad (4)$$

where k is the shape parameter. When $k = 1$, the time interval distribution reduces to the exponential distribution; when $k < 1$, the bursts are clustered; and when $k > 1$, the bursts tend to be periodic. A detailed discussion about the time interval distribution is shown in the Appendix.

For non-repeating FRBs, to be detectable, they should also exceed the threshold energy shown in Equation 1.

Assume that the energy of non-repeating FRBs follow a simple power-law distribution as

$$\frac{dN}{dE} \propto E^{-\gamma_n} \quad (5)$$

with $E_0 < E < E_{\text{max}}$. We adopt the same E_0 and E_{max} values as Equation 2 and take $\gamma_n = 1.8$ ([Luo et al. 2020](#); [Lu & Piro 2019](#))¹.

We assume that the lifetimes of the repeaters are much longer than the observational timescale. In a steady state, the birth rate and the death rate of the repeating sources would balance each other, so that the total number of sources in the sky would be a constant. We also assume that the repeating rate distribution remains the same during the observing period so that we do not consider the evolution of the repeating sources and their population properties.

For genuine non-repeating sources, the progenitor of the FRB produces an FRB once in its lifetime. The number of non-repeating sources accumulate linearly with time with a constant event rate density. Let us denote the total number of repeating sources in the universe as N_r and the total event rate of non-repeating FRBs in the universe as \dot{N}_n . One can define a characteristic timescale

$$T_c \equiv \frac{N_r}{\dot{N}_n}, \quad (6)$$

at which the number of repeating and non-repeating sources in the sky become comparable².

Depending on the effective repeating rate r , a repeating source may be recognized as a repeater (if r is large enough), an apparent non-repeater (if r is smaller), or not detected at all (if r is extremely small). We use f_{rr} and f_{rn} to denote the fractions of repeating sources being recognized as repeating and non-repeating sources, respectively. For non-repeating sources, only a fraction, f_{nn} , are detected with a fluence above F_{th} . Therefore, for a sample of observed FRB sources, the fraction of identified repeating sources among all the detected sources should be

$$\begin{aligned} F_{\text{r,obs}}(t) &= \frac{f_{\text{rr}}(t) N_r \frac{\Omega}{4\pi}}{f_{\text{rr}}(t) N_r \frac{\Omega}{4\pi} + f_{\text{rn}}(t) N_r \frac{\Omega}{4\pi} + f_{\text{nn}} \dot{N}_n t \frac{\Omega'}{4\pi}} \\ &= \frac{f_{\text{rr}}(t)}{f_{\text{rr}}(t) + f_{\text{rn}}(t) + f_{\text{nn}} \frac{t}{T_c} \frac{\Omega'}{\Omega}}, \end{aligned} \quad (7)$$

¹ For both non-repeaters and repeaters, the energy of some bursts could be in principle below E_0 . For the observational configurations we simulate (similar to that of CHIME), these low-energy bursts are not detectable at cosmological distances.

² One may also define $T_c \equiv \rho_r / \dot{\rho}_n$, where ρ_r is the local density of repeating sources and $\dot{\rho}_n$ as the local event rate density of non-repeating sources. The following discussion remains the same if the redshift distributions of the repeating sources and the non-repeating sources are roughly the same.

which is a function of the observational time t . Here Ω' is the field of view of the telescope, and Ω is the total sky solid angle the telescope can cover.

3. MONTE CARLO SIMULATIONS

In this section, we use Monte Carlo simulations to estimate f_{rr} , f_{rn} and f_{nn} and then predict the observed fraction of repeating bursts $F_{r,obs}(t)$ at a certain observational time t . The results depend on several parameters, such as T_c , r_0 , and F_{th} . The main procedure of our simulations include the following six steps:

- Generate a series of repeating sources with a certain redshift distribution.
- Calculate the effective repeating rate for each simulated repeating source.
- Generate burst time intervals according to the Weibull distribution (given a particular k value) and form a time sequence of the repeated bursts from each repeating FRB source.
- Set an observational configuration (e.g. mimic CHIME) and estimate the values of f_{rr} and f_{rn} .
- Generate a population of non-repeating sources with a certain redshift distribution model and energy distribution model. Then estimate the value of f_{nn} .
- Substitute f_{rr} , f_{rn} and f_{nn} into equation 7 and calculate $F_{r,obs}$ as a function of time.

In our simulations, we assume that the redshift distributions for both repeating and non-repeating sources follow the star formation rate (SFR) history. We adopt an analytical fitting formula given by [Yüksel et al. \(2008\)](#)

$$\text{SFR}(z) \propto \left[(1+z)^{3.4\eta} + \left(\frac{1+z}{5000} \right)^{-0.3\eta} + \left(\frac{1+z}{9} \right)^{-3.5\eta} \right]^{1/\eta} \quad (8)$$

where $\eta = -10$. We generate N_r redshift values according to Equation 8 and assign each value to one repeating FRB source. Choosing appropriate values of F_{th} and r_0 , for each repeater, we could calculate its effective repeating rate r using Equation 1 - 3.

Assume the observation starts from T_0 . A waiting time needs to be introduced to describe how long it takes to detect the first burst from each source. In our simulations, we randomly generate a time interval δ_1 according to Equation 4 and then randomly generate a waiting

time t_w in the range of $[0, \delta_1]^3$. Hence, the first burst appears at $T_1 = T_0 + t_w$. For the sake of convenience, we set $T_0 = 0$. For each repeating source, we simulate N bursts, which appear at $T_i = T_1 + \sum_{j=2}^i \delta_j$ where $i = 1, 2, 3 \dots N$. Those bursts that fall into the field of view of a telescope at the burst time would be detected if it is above the flux threshold.

In reality, the telescope may not stare at one particular sky area all the time. Therefore, for each repeating source, the observation is not continuous, but consists of a number of discrete short-term observations. We assume t_e as the duration of each observation at a certain sky area, and t_g as the gap between two observations at the same area. For an observing time t ($t < T_{i=N}$) for a telescope, there are $n = t/(t_e + t_g)$ observing periods. From a simulation, we count the number of T_i 's for each source that satisfy $m(t_e + t_g) < T_i < t_e + m(t_e + t_g)$, where $m = 0, 1, 2 \dots n-1$. If more than one burst was detected, it would be recognized as a repeater; if exactly one burst was detected, it would be recognized as an apparently non-repeating source; otherwise, the source would not be detected. Investigating all the sources in the simulation, we can obtain the values of f_{rr} and f_{rn} .

Non-repeating sources are generated following the redshift (Equation 8) and energy (Equation 5) distributions. The fraction f_{nn} could be estimated through dividing the number of detectable non-repeating bursts by the total number of simulated non-repeating sources. Note that f_{nn} is not a function of time.

In our simulations, we take the threshold fluence as $F_{th} = 4$ Jy ms, which is comparable to CHIME's sensitivity ([CHIME/FRB Collaboration et al. 2019b](#); [Fonseca et al. 2020](#)). We generate 10^6 non-repeating sources and $f_{nn} \sim 0.005$ can be determined. According to our definition, the total solid angle Ω covered by the telescope would be observed once in $t_e + t_g$, and t_e is the effective observational time for the field of view with a solid angle Ω' . We then have $\Omega'/\Omega = nt_e/t$. Equation 7 can be then rewritten as

$$F_{r,obs} = \frac{f_{rr}(t)}{f_{rr}(t) + f_{rn}(t) + f_{nn} \frac{nt_e}{T_c}} \quad (9)$$

4. RESULTS

4.1. Evolution of $F_{r,obs}$

Our first goal is to investigate how the observed repeater fraction, $F_{r,obs}$, evolves with time, and how this evolution depends on the parameter T_c , a characteristic parameter to define the relative fractions between the

³ When $k = 1$ in Equation 4 is assumed, the distribution of t_w is the same as that of δ .

genuine repeaters and non-repeaters: $T_c \rightarrow \infty$ means all FRBs are repeaters, and $T_c \rightarrow 0$ means that the majority FRBs are genuine non-repeaters.

We first give an example by assuming that all repeaters are as active as the first repeating source FRB 121102 ($r_0 = 0.1 \text{ hr}^{-1}$) (Law et al. 2017; James 2019). The observed fraction of repeating sources $F_{r,\text{obs}}$ as a function of observational time t is shown in Figure 1. For $T_c \rightarrow \infty$, $F_{r,\text{obs}}$ always increases, but the slope decreases as a function of time. If T_c is a finite value, which means there are genuine non-repeating sources, $F_{r,\text{obs}}$ increases with time first because of the fast increasing of f_{rr} in the beginning. Later on, the increase of f_{rr} slows down because one already recognizes most of the repeaters. On the other hand, the number of non-repeating sources linearly increases with time, so that $F_{r,\text{obs}}$ would reach a peak and then starts to decrease afterwards.

In the following, we denote the expected maximum fraction of repeating sources as the “peak fraction” ($F_{r,\text{obs},p}$) and its corresponding time is expressed as the “peak time” (T_p).

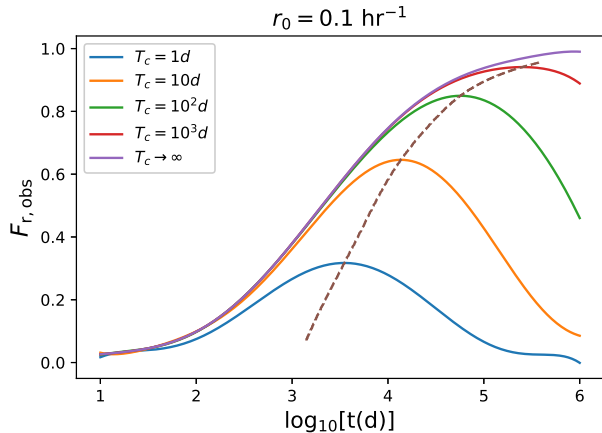


Figure 1. The observed repeater fraction $F_{r,\text{obs}}$ as a function of time. The colored solid lines delineate the evolution of $F_{r,\text{obs}}$ for different T_c values. The dashed line marks the trajectory of the peak fraction vs. peak time as a function of T_c . Following parameters are adopted: $t = n(t_e + t_g)$, where $t_e = 0.2 \text{ hr}$ and $t_g = 23.8 \text{ hr}$; the Weibull parameter is adopted as $k = 1$.

From Figure 1, we can see that the distinction of $F_{r,\text{obs}}$ curves for different T_c 's is insignificant when t is short. A distinct feature occurs around the peak time. The peak time and peak fraction are the most crucial observational quantities that can be used to estimate T_c . A smaller T_c corresponds to a more dominant non-repeater population, which corresponds to a smaller peak time and a lower peak fraction.

4.2. Effect of key parameters

As already known from section 4.1, with a fixed r_0 , T_c is a parameter that strongly influences T_p and $F_{r,\text{obs},p}$. In this section, we allow the value of r_0 vary among repeating FRBs to get more realistic results.

We consider that the values r_0 for different sources follow a power-law distribution, i.e.

$$\frac{dn^*}{dr_0} \propto r^{-q}, \quad (10)$$

where dn^* represents the number of repeating sources with the intrinsic repeating rate in the range of $r_0 \sim r_0 + dr_0$. For this distribution, one can introduce three parameters: two for the r_0 range ($r_{0,\text{min}}$ and $r_{0,\text{max}}$), and one for the power-law index (q). Among these three parameters, $r_{0,\text{max}}$ is the most accessible one, which could be directly measured from the most active repeating sources in the universe (e.g. active repeaters at a relatively large distance). The index q can also be obtained observationally by fitting the repeaters' repetition rate distribution. However, the value of $r_{\text{min},0}$ is much more difficult to determine, because observationally it is hard to distinguish a repeating source with a very low r_0 from an intrinsically non-repeating burst.

In our simulation, we adopt a fixed maximum repeating rate $r_{0,\text{max}} = 10^{0.5} \text{ hr}^{-1}$, which is obtained by fitting CHIME's latest repeating FRB sample (Lu et al. 2020). We then choose different $r_{0,\text{min}}$ and q values to see how they influence the simulation results. We fix one of these two parameters and vary the other one in every simulation. The results are shown in Figure 3 with solid lines denote the locus of $(T_p, F_{r,\text{obs},p})$ as the parameters are varied. When we set a fixed index as $q = 1.6$ and vary the value of $r_{0,\text{min}}$, the results are shown in the left panel of Figure 3. With the same T_c , a lower $r_{0,\text{min}}$ would lead to a smaller $F_{r,\text{obs},p}$ and a smaller T_p . When we set $r_{0,\text{min}} = 10^{-5.5} \text{ hr}^{-1}$ and vary the value of q , the results are shown in the right panel of Figure 3. With the same T_c , a higher q would lead to a smaller $F_{r,\text{obs},p}$ and a smaller T_p .

Both a lower $r_{0,\text{min}}$ and a higher q would make more repeating sources with low r_0 values. Consider that the increase of f_{rr} slows down when most of the sources which repeat frequently enough have been recognized as repeating sources. If there are more low r_0 sources, f_{rr} would have a smaller absolute value and its increase rate would become smaller. This explains why both $F_{r,\text{obs},p}$ and T_p become smaller in these cases.

In Figure 3, we also allow that the shape parameter k for Weibull distribution to vary in different simulations. We find that the k value would dramatically influence

the peak time but only slightly influence the peak fraction when other parameters are set to fixed values.

4.3. Constraint on T_c

Four parameters (T_c , $r_{0,\min}$, q and k) have been discussed in the previous sections. The latter three parameters are related to repeating sources only, which may be eventually measured from the observations of repeaters. The T_c parameter concerns the true relative fractions of repeaters and non-repeaters, which cannot be measured directly from the repeater data only. It may, however, be constrained from the observed $F_{r,\text{obs}}$ as a function of time, or the measurement of $(T_p - F_{r,\text{obs},p})$ if a peak indeed exists. In principle, for a reasonable k range (e.g. from 0.3 to 1), once a peak is detected, one may find an appropriate r_0 distribution to make the observed peak point located in region of the predicted peak points within the assumed k range (contours in Figure 3). Finding the T_c contour line that goes through the observed peak point, one can then determine both T_c and k . In reality, there might not be only one r_0 distribution that can satisfy the observational constraint. Hence, constraints on r_0 distribution from the repeating FRB data would be helpful to make more stringent constraints on T_c .

Since $F_{r,\text{obs},p}$ is insensitive to the k parameter (see nearly horizontal T_c contours in Figure 3), when a peak is measured, one may use $F_{r,\text{obs},p}$ to roughly constrain T_c if other parameters ($r_{0,\min}$, $r_{0,\max}$, and q) are constrained from the repeater data. Figure 3 shows how $F_{r,\text{obs},p}$ depends on T_c for different sets of repeating burst parameters. The solid and dashed lines show the range of k from 0.3 to 1. These figures can be used to estimate T_c directly.

According to our simulations, depending on parameters T_p can be much longer than the observational timescale, e.g. up to thousands of years. In general, even when the peak (if exists), i.e. $(T_p, F_{r,\text{obs},p})$, has not been detected yet, one can still put constraints on T_c . Similar to the case with an observed peak, one can also find the T_c value corresponding to the current $F_{r,\text{obs}}$ and observational time t . This T_c value would serve as the lower limit, since Both $F_{r,\text{obs},p}$ and T_p increase with T_c . In the case when $F_{r,\text{obs}}$ and t do not appear in the solid T_c contour region in Figure 3, we also plot the conservative constraints on T_c with dashed lines in Figure 3. The observational run by CHIME from 2018 August 28 to 2019 September 30 has detected ~ 700 new FRBs with 9 repeaters (Fonseca et al. 2020). We thus place the fraction 0.013 with 400 d observation in each panel of Figure 3 to denote the current data constraint.

In Table 1, we summarize the constraints on T_c with some characteristic T_p (t) and $F_{r,\text{obs},p}$ ($F_{r,\text{obs}}$) values for the assumed range of k . The boldface numbers are the T_c values for which the measured t and $F_{r,\text{obs}}$ roughly correspond to T_p and $F_{r,\text{obs},p}$, respectively. Other numbers are the lower limits of T_c for the corresponding observable t and $F_{r,\text{obs}}$. If the peak has not been detected yet, one can only place a lower limit on T_c with the current data. With all the parameter sets adopted in this paper and assuming that the current $F_{r,\text{obs}} = 0.013$ given by CHIME (Fonseca et al. 2020) is a lower limit, we find that $T_c > (0.5 - 25)$ d. That means that in a one-year period, the real fraction of the repeating sources in the universe should be $F_r(1\text{yr}) = 1/(1 + 1\text{yr}/T_c) > (0.0014 - 0.060)$. In the future, if a larger $F_{r,\text{obs}}$ is observed, one should be able to place a more stringent constraint on T_c . For example, if $F_{r,\text{obs}} > 0.1$ has been observed, one would have $T_c > (7 - 870)$ d, which means $F_r(1\text{yr}) > (0.018 - 0.7)$; If $F_{r,\text{obs}} > 0.2$ has been observed, one would have $T_c > (26 - 670)$ d, which means $F_r(1\text{yr}) > (0.067 - 0.65)$; If $F_{r,\text{obs}} > 0.3$ has been observed, one would have $T_c > (78 - 3500)$ d, which means $F_r(1\text{yr}) > (0.18 - 0.91)$. In any case, only when a peak $F_{r,\text{obs},p}$ has been detected, would the ansatz that all FRB sources repeat be disfavored, and an upper limit on T_c can be obtained.

5. CONCLUSIONS AND DISCUSSION

We have introduced a parameter T_c (defined in Equation 6) to describe the real fraction of repeating FRB sources in the entire universe. A smaller T_c means a larger fraction of genuinely non-repeating sources per unit time. The ansatz that all FRBs repeat corresponds to $T_c \rightarrow \infty$.

Consider that not all repeating sources can be recognized, we performed a set of Monte Carlo simulations to investigate how the observed repeating source fraction $F_{r,\text{obs}}$ is related to the true fraction (T_c as a proxy). We found that once a finite T_c is introduced, $F_{r,\text{obs}}$ would not always increase with time, but instead shows a turnover after reaching a peak value $F_{r,\text{obs},p}$ at a peak time T_p . The expected turnover point is highly dependent on T_c , with a larger T_c corresponding to a higher $F_{r,\text{obs},p}$ and a later T_p .

The $(T_p, F_{r,\text{obs},p})$ pair also depends on the repeating rate distribution of the repeaters as well as time distribution function of the bursts (the Weibull parameter k). We assume that the intrinsic repeating rate r_0 satisfies a power-law distribution with an index q in the range of $[r_{0,\min}, r_{0,\max}]$. We fix $r_{0,\max}$ (which could be measured from known repeaters) and investigate the other the effects of the other two parameters. We found

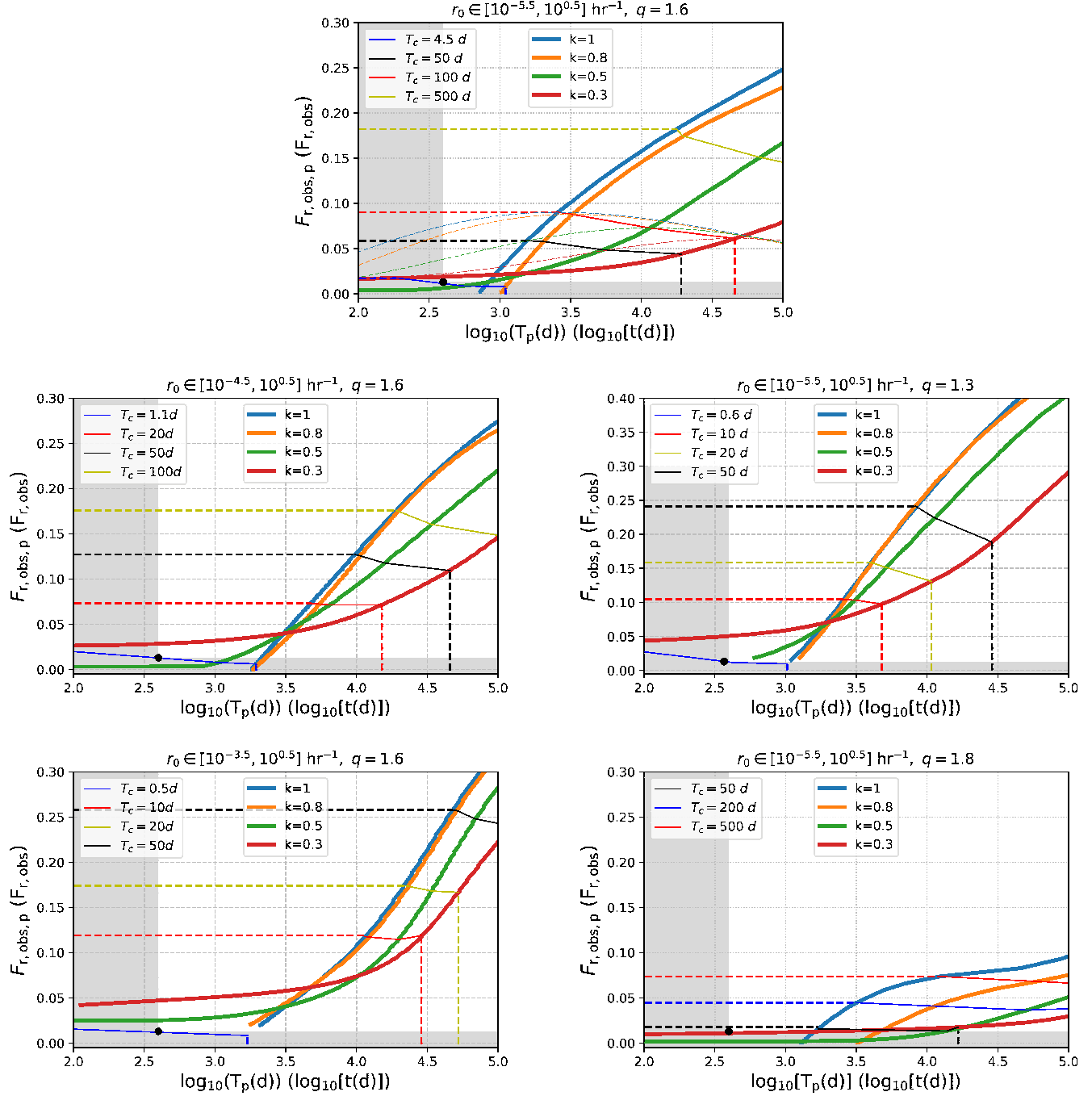


Figure 2. Observed peak repeater fraction and peak time ($T_p - F_{r, obs, p}$) of repeating FRB sources for different model parameters. All the figures allow an r_0 distribution among repeating FRB sources, with different r_0 distribution range and q values marked on the top of each panel. Thick solid lines stand for the locus ($T_p, F_{r, obs, p}$) when different T_c (thin solid color contours) and k values (thick solid color lines) are assumed. Dashed lines are the most conservative constraints on T_c through the observational time t and observed fraction $F_{r, obs}$ before a peak is reached. In the upper panel, the dot-dashed lines show the evolution of $F_{r, obs}$ as a function of time as examples. The black dot in each figure stands for the current observational time and fraction of repeating sources according to the CHIME results (Fonseca et al. 2020). All five figures assume that $t = n(t_e + t_g)$, where $t_e = 0.2$ hr and $t_g = 23.8$ hr.

that a higher q and a lower $r_{0, min}$ would both result in a

distribution with more inactive repeating sources, which

$q = 1.6$

		$r_{0,\min} = 10^{-5.5}\text{hr}^{-1}$				$r_{0,\min} = 10^{-4.5}\text{hr}^{-1}$				$r_{0,\min} = 10^{-3.5}\text{hr}^{-1}$			
T_c (d)	$F_{\text{r,obs}} (\mathbf{F}_{\text{r,obs,p}})$	0.013	0.1	0.2	0.3	0.013	0.1	0.2	0.3	0.013	0.1	0.2	0.3
$t (\mathbf{T_p})$													
400 d		4.5	120	670	3500	1.1	35	140	550	0.5	7	26	78
3 yr		9	120	670	3500	2	35	140	550	0.6	7	26	78
10 yr		×	125	670	3500	×	35	140	550	×	7	26	78
30 yr		×	155	670	3500	×	35	140	550	×	7	26	78

$r_{0,\min} = 10^{-5.5}\text{hr}^{-1}$

		$q = 1.3$				$q = 1.8$			
T_c (d)	$F_{\text{r,obs}} (\mathbf{F}_{\text{r,obs,p}})$	0.013	0.1	0.2	0.3	0.013	0.1	0.2	0.3
$t (\mathbf{T_p})$									
400 d		0.6	9	35	300	25	870	—	—
3 yr		1	9	35	300	25	870	—	—
10 yr		×	9.5	35	300	45	870	—	—
30 yr		×	×	45	300	50	870	—	—

Table 1. T_c lower limits (or its values in the case of boldface) calculated from the observation time t and its corresponding $F_{r,\text{obs}}$ (or the corresponding peak time T_p and peak fraction $F_{r,\text{obs,p}}$ in the case of boldface). The “×” signs mean that the set of t and $F_{r,\text{obs}}$ are not possible with the corresponding r_0 -distribution parameters assumed. With the same r_0 , k and r_0 distribution, the case with a higher T_c value would always have a higher $F_{r,\text{obs}}$. If an evolution curve is supposed to reach a peak somewhere in the region enclosed by the solid lines in Figure 3, it may never enter the region below the lowest thick solid lines. The “—” signs stand for the case of $t > 10^6$ d in our simulations, which are observationally unattainable.

would lead to a lower $F_{r,\text{obs,p}}$ and earlier T_p . With other parameters fixed, the k parameter would dramatically influence T_p but only slightly change $F_{r,\text{obs,p}}$. Hence, one can use $F_{r,\text{obs,p}}$ to constraint T_c independent of the k value, if r_0 distribution is well constrained.

Available CHIME observations gives $F_{r,\text{obs}} \sim 0.013$ at $t \sim 400$ d. If this is a lower limit, the data can already place a lower limit on T_c , i.e. $T_c > (0.5 - 25)$ d. In the future, if higher value of $F_{r,\text{obs}}$ is observed, a more stringent lower limit on T_c can be obtained. However, only when a peak is actually observed can one derive an up-

per limit on T_c . The ansatz that all FRB sources repeat cannot be disfavored until such a peak is detected.

ACKNOWLEDGMENTS

SA and BZ acknowledges the Top Tier Doctoral Graduate Research Assistantship (TTDGRA) at University of Nevada, Las Vegas for support. HG acknowledges the National Natural Science Foundation of China (NSFC) under Grant No. 11722324, 11690024 and the Fundamental Research Funds for the Central Universities for support. BZ thanks Xuelei Chen for a stimulative conversation.

REFERENCES

- Caleb, M., Stappers, B. W., Rajwade, K., & Flynn, C. 2019, MNRAS, 484, 5500, doi: [10.1093/mnras/stz386](https://doi.org/10.1093/mnras/stz386)
- CHIME/FRB Collaboration, Amiri, M., Bandura, K., et al. 2019a, Nature, 566, 235, doi: [10.1038/s41586-018-0864-x](https://doi.org/10.1038/s41586-018-0864-x)
- CHIME/FRB Collaboration, Andersen, B. C., Bandura, K., et al. 2019b, ApJL, 885, L24, doi: [10.3847/2041-8213/ab4a80](https://doi.org/10.3847/2041-8213/ab4a80)
- Cordes, J. M., & Chatterjee, S. 2019, ARA&A, 57, 417, doi: [10.1146/annurev-astro-091918-104501](https://doi.org/10.1146/annurev-astro-091918-104501)
- Fonseca, E., Andersen, B. C., Bhardwaj, M., et al. 2020, ApJL, 891, L6, doi: [10.3847/2041-8213/ab7208](https://doi.org/10.3847/2041-8213/ab7208)
- James, C. W. 2019, MNRAS, 486, 5934, doi: [10.1093/mnras/stz1224](https://doi.org/10.1093/mnras/stz1224)
- Law, C. J., Abruzzo, M. W., Bassa, C. G., et al. 2017, ApJ, 850, 76, doi: [10.3847/1538-4357/aa9700](https://doi.org/10.3847/1538-4357/aa9700)
- Lorimer, D. R., Bailes, M., McLaughlin, M. A., Narkevic, D. J., & Crawford, F. 2007, Science, 318, 777, doi: [10.1126/science.1147532](https://doi.org/10.1126/science.1147532)

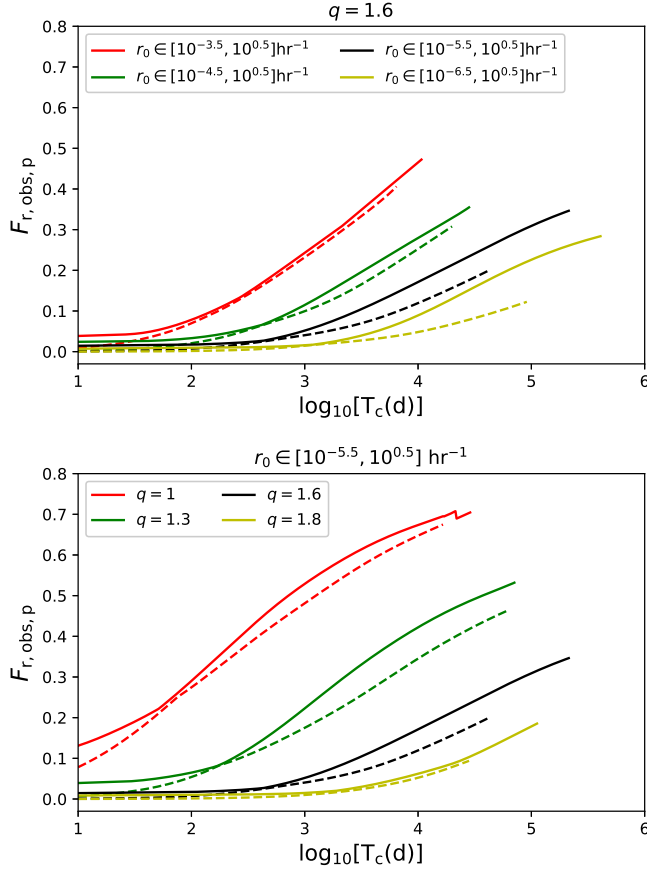


Figure 3. $F_{r,obs,p}$ as a function of T_c . The solid and dashed lines represent the upper and lower limit of $F_{r,obs,p}$ in the range of k (from 0.3 to 1), respectively. Other parameters are the same as those in Figure , as shown in the labels in the plots.

- Lu, W., & Piro, A. L. 2019, ApJ, 883, 40, doi: [10.3847/1538-4357/ab3796](https://doi.org/10.3847/1538-4357/ab3796)
- Lu, W., Piro, A. L., & Waxman, E. 2020, arXiv e-prints, arXiv:2003.12581. <https://arxiv.org/abs/2003.12581>
- Luo, R., Lee, K., Lorimer, D. R., & Zhang, B. 2018, MNRAS, 481, 2320, doi: [10.1093/mnras/sty2364](https://doi.org/10.1093/mnras/sty2364)
- Luo, R., Men, Y., Lee, K., et al. 2020, MNRAS, 494, 665, doi: [10.1093/mnras/staa704](https://doi.org/10.1093/mnras/staa704)
- Oppermann, N., Yu, H.-R., & Pen, U.-L. 2018, MNRAS, 475, 5109, doi: [10.1093/mnras/sty004](https://doi.org/10.1093/mnras/sty004)
- Palaniswamy, D., Li, Y., & Zhang, B. 2018, ApJL, 854, L12, doi: [10.3847/2041-8213/aaaa63](https://doi.org/10.3847/2041-8213/aaaa63)
- Petroff, E., Hessels, J. W. T., & Lorimer, D. R. 2019, A&A Rv, 27, 4, doi: [10.1007/s00159-019-0116-6](https://doi.org/10.1007/s00159-019-0116-6)
- Petroff, E., Johnston, S., Keane, E. F., et al. 2015, MNRAS, 454, 457, doi: [10.1093/mnras/stv1953](https://doi.org/10.1093/mnras/stv1953)
- Ravi, V. 2019, Nature Astronomy, 3, 928, doi: [10.1038/s41550-019-0831-y](https://doi.org/10.1038/s41550-019-0831-y)
- Spitler, L. G., Scholz, P., Hessels, J. W. T., et al. 2016, Nature, 531, 202, doi: [10.1038/nature17168](https://doi.org/10.1038/nature17168)
- Thornton, D., Stappers, B., Bailes, M., et al. 2013, Science, 341, 53, doi: [10.1126/science.1236789](https://doi.org/10.1126/science.1236789)
- Yüksel, H., Kistler, M. D., Beacom, J. F., & Hopkins, A. M. 2008, ApJL, 683, L5, doi: [10.1086/591449](https://doi.org/10.1086/591449)

APPENDIX

A. WEIBULL DISTRIBUTION

The distribution of the time interval of two adjacent bursts in a repeating source could be describe by a Wellbull function, which reads

$$\mathcal{W}(\delta|k, r) = k\delta^{-1} [\delta r \Gamma(1 + 1/k)]^k e^{-[\delta r \Gamma(1 + 1/k)]^k}, \quad (\text{A1})$$

where r represents the mean repeating rate, k is the shape parameter, and $\Gamma(x)$ stands for the Gamma function.

When $k = 1$, the distribution is reduced to the exponential (i.e. Poisson) distribution. In this case, Equation A1 is simplified as

$$\mathcal{W}(\delta|r) = r e^{-r\delta}. \quad (\text{A2})$$

The mean interval time is

$$\langle \delta \rangle = \int_0^\infty \delta \mathcal{W}(\delta|r) d\delta = 1/r. \quad (\text{A3})$$

The variance of δ could be calculated as

$$\begin{aligned} D(\delta) &= \langle \delta^2 \rangle - \langle \delta \rangle^2 \\ &= \int_0^\infty \delta^2 \mathcal{W}(\delta|r) d\delta - \frac{1}{r^2} \\ &= \frac{2}{r^2} - \frac{1}{r^2} \\ &= \frac{1}{r^2}. \end{aligned} \quad (\text{A4})$$

Assume that an observation starts at time t_s after the first burst and the waiting time until the next burst appears is t_w . The probability that an observer would wait for at least a period of t_1 could be written as

$$\begin{aligned} P(t_w > t_1) &= P(\delta > t_s + t_1 | \delta > t_s) = \frac{e^{-r(t_1 + t_s)}}{e^{-rt_s}} \\ &= e^{-rt_1}. \end{aligned} \quad (\text{A5})$$

Similarly, the probability of having a burst in t_1 would be

$$P(t_w < t_1) = 1 - e^{-rt_1}, \quad (\text{A6})$$

which is independent of t_s . The probability density function is

$$\mathcal{W}(t_w|r) = r e^{-rt_w}, \quad (\text{A7})$$

which is the same as that of the time interval δ . Therefore, the mean waiting time is the same as the true mean interval time between two adjacent bursts.

When $k \neq 1$, one can similarly calculate the mean time interval as

$$\begin{aligned} \langle \delta \rangle &= \int_0^\infty \delta \mathcal{W}(\delta|r) d\delta \\ &= \int_0^\infty k [\delta r \Gamma(1 + 1/k)]^k e^{-[\delta r \Gamma(1 + 1/k)]^k} d\delta \\ &= \frac{1}{r \Gamma(1 + 1/k)} \int_0^\infty x^{1/k} e^{-x} dx, \end{aligned} \quad (\text{A8})$$

where $x = [\delta r \Gamma(1 + 1/k)]^k$. Considering that $\Gamma(1 + z) = \int_0^\infty x^z e^{-x} dx$, one has

$$\langle \delta \rangle = \frac{1}{r \Gamma(1 + 1/k)} \times \Gamma(1 + 1/k) = \frac{1}{r}. \quad (\text{A9})$$

The mean time interval does not change with k .

We can calculate the variance of the Weibull distribution to study the clustering effect introduced by the shape parameter k . The variance is

$$\begin{aligned} D(\delta) &= \langle \delta^2 \rangle - \langle \delta \rangle^2 \\ &= \int_0^\infty \delta^2 \mathcal{W}(\delta|r) d\delta - \frac{1}{r^2} \\ &= \frac{1}{[r \Gamma(1 + 1/k)]^2} \int_0^\infty x^{2/k} e^{-x} dx - \frac{1}{r^2} \\ &= \frac{1}{r^2} \left[\frac{\Gamma(1 + 2/k)}{\Gamma(1 + 1/k)^2} - 1 \right]. \end{aligned} \quad (\text{A10})$$

Compared with exponential distribution, the variance of Weibull distribution is corrected by a factor

$$f(k) = \frac{\Gamma(1 + 2/k)}{\Gamma(1 + 1/k)^2} - 1 \quad (\text{A11})$$

as a function of k , which is shown in Figure 4.

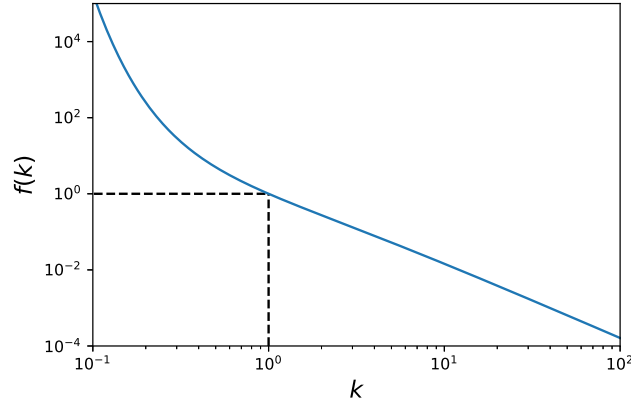


Figure 4. The correcting factor $f(k)$ of the variance of Weibull distribution compared with exponential distribution as a function of shape parameter k .

When $k < 1$, the variance of Weibull distribution is larger than $1/r^2$, which means that both longer and shorter time intervals have more chance to appear. That would lead to the case that some bursts are closer to each other and some others are more separated from each other. Hence we tend to detect “clusters” of bursts. When $k > 1$, the variance of Weibull distribution would be smaller than $1/r^2$, which means that the time intervals between bursts tend to be the same. In this case, the repeating burst would appear to be more “periodic”.

In addition, when $k \neq 1$, the waiting time distribution is not the same as the time interval distribution.